Mechanical Properties of Silver Nanoparticles Induced Europium Doped Phosphate Glasses for Red Laser Application

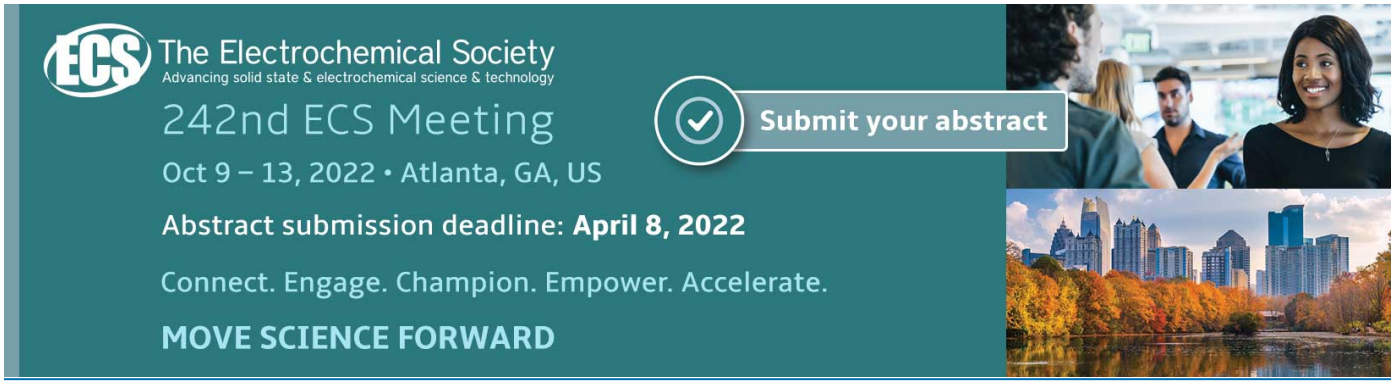

Mechanical Properties of Silver Nanoparticles Induced Europium Doped Phosphate Glasses for Red Laser Application

I.M. Danmallam[1,3], H Bakhtiar[1,2], A.A.Salim[2] , I Bulus[1,4], S K Ghoshal[*1,2]

[1]AOMRG, Department of Physics, Faculty of Science, Universiti Teknologi Malaysia, 81310 Skudai, Johor, Malaysia.
[2]Laser Centre and Advance Optical Materials Research Group,Department of Physics, Faculty of Science, Universiti Teknologi Malaysia, 81310 Skudai, Johor, Malaysia.
[3]Sokoto Energy Research Center, Usmanu Danfodiyo University Sokoto, Sokoto, Nigeria.
[4]Department of Physics, School of Sciences, Kaduna State College of Education Gidan waya, Kafanchan, Nigeria.

Email: sibkrishna@utm.my, ibrahimdanmallam @gmail.com

ABSTRACT. Magnesium-zinc-sulfophosphate glasses with varying concentration of Silver nanoparticles (AgNPs) composition of $63.5P_2O_5$–20MgO –$15ZnSO_4$–$1.5Eu_2O_3$ –zAgNps (z = 0.0, 0.1, 0.3, 0.5, 0.7,0.9 and 1.1 g in excess) was prepared using melt-quenching technique. The as-Quenched glass samples were characterised to ascertain the correlation between physical and mechanical characteristics. The enhanced Young's, shear, and bulk modulus of glasses noted a comparative rise in AgNPs contents. The Poisson's ratio improved from (0.0978 to 0.1416) while Vickers hardness (from 0.0658 to 0. 0.0682 GPa) as well as GC_{12} (from 0.8350 to 0.8916) were enhanced. Photoluminescence spectra (emission) of the glasses showed four peaks at 593, 613, 654, and 701 nm equivalent to $^5D_0 \rightarrow {}^7F_0$, $^5D_0 \rightarrow {}^7F_2$, $^5D_0 \rightarrow {}^7F_3$, and $^5D_0 \rightarrow {}^7F_4$ transitions in europium in which the intense peak was observed at 613 nm (red). High Quantum Efficiency ($\eta = 97.9\%$) was achieved due to significant PL enhancement. The studied glass may be useful for the development of red laser

1.Introduction

In recent times, oxide glasses have received wide attention largely due to the superior mechanical properties of these alloys, which include high elastic strain limit, high hardness, abrasion resistance, and great strength [1]. The mechanical properties of glass are dependent on microstructure and phase crystalline assembly [2]). The hardness of glass materials usually implied as resistance to abrasion and scratching [3]. Glass properties vary significantly with chemical composition. Rare-earth doped glasses performed substantial character in developing biocompatible appliances [4]. Microscopic cracks or surface layer defects determine glass strength [5]. Exceptional properties of glass, such as high resistance, high hardness, and low toughness fracture, have led to the manifold technological application [6].

Phosphate has excellent features such as higher density and lower refractive index[7][8]. Europium improves the absorption property of phosphors (around 400 nm), thereby improving the photoluminescence feature[9] [10]. A suitable method of studying small volume materials' mechanical features is via indentation hardness, where a fixed load on the diamond indenter is applied and measured using a microscope. Vickers hardness is the most widely used among several geometry indenters in hardness testing. The diamond pyramid hardness number *HV* is the ratio of applied load to contact surface (area). A low load hardness test was conducted with the load levels ranging from 5 to 50 N with a dwell period of 30 seconds [11].

Silver nanoparticles improve luminescence intensity and display attractive optical sensations of nonlinear features [10]. Energy transfer between REI and NPs present a positive viewpoint for solid-state lighting application [11]. The interaction of silver nanoparticles with the host matrix (at the metal-dielectric interface) induces a high electric field in the rare earth ions vicinity [12]. Overcoming these complications, glasses were sensitized with minute silver nanoparticles in other to alter the dielectric

environment of the dopant [13]. Photoluminescence improvement occurs as a result of the confinement of electromagnetic field initiating from the local field environment of AgNPs due to vigorous light absorption by silver nanoparticles [14].

Considering the benefits, this study evaluates the mechanical traits of phosphate glass. The glasses were synthesized by the melt-quenching technique and analyzed with several investigative instruments.

2.Experimental Procedures

Reagents from Sigma Aldrich were used as raw materials for the synthesis of glasses with molar concentration $63.5P_2O_5$–$20MgO$ –$15ZnSO_4$–$1.5Eu_2O_3$ –yAgNps (y = 0.0, 0.1, 0.3, 0.5, 0.7, 0.9 and 1.1 g in excess). 15 g of batch composition was placed in crucible then placed in a furnace (1100 °C) for 90 minutes. Samples were analysed using RIGOL DS202 digital oscilloscope and Vickers indenter.

3.Physical Traits of the Studied Glasses

Densities increased (from 3.0720 to 4.3304 g/cm^3) due to large molecular mass Eu_2O_3 than that of phosphate. The decrease in density might be attributed to the Eu^{3+} ions taking part in the glass structure. Figure 1 shows a decrease in molar volume ranged (from 43.5682 to 30.8883 cm^3) with a proportionate increase in AgNPs contents. The inverse trend of molar volume to density is due to a change in structure with increased compactness and rigidity of the glasses [12]. Molar volume decrease shows an increase in oxygen packing density and shrinkage of bond length [9].

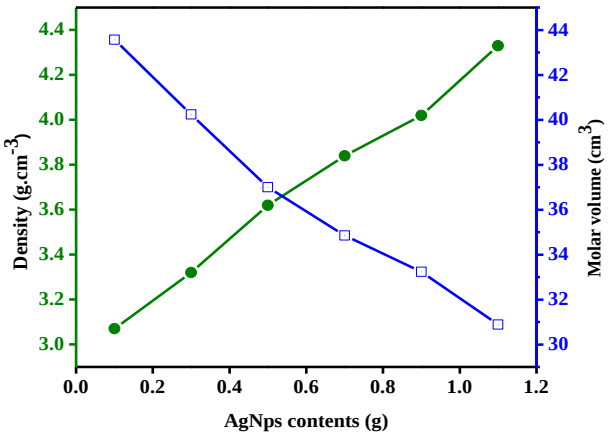

Figure. 1 Density and Molar Volume Against AgNPs Contents

3.1Mechanical Properties

Mechanical properties of glass are dependent on microstructure and phase crystalline assembly. The hardness of glass materials usually implied as resistance to abrasion and scratching [3]. Glass properties vary significantly with their chemical composition [4]. Microscopic cracks or surface layer defects determine glass strength [5]. Exceptional quantum efficiency and the high branching ratio of the glass system signify the high potential for red laser application [6].

A suitable method of studying mechanical properties of small-volume materials is via indentation hardness, where a fixed load on the diamond indenter is applied and measured using a microscope. Vickers hardness is the most widely used among several geometry indenters in hardness testing. The diamond pyramid hardness number HV is the ratio of applied load to contact surface (area). Low load hardness tests were conducted with load levels of 50 N with a dwell period of 30s [11]. The CIE color chromaticity was evaluated. The embedment of Ag Nps to determine the lasing potency and optical enhancement was performed. In general, Eu^{3+} doped glasses display several potential applications in red phosphors, color display, LED, and solid-state laser due to its narrowband

emission at 614nm (red emission) attributed to $^5D_0 \rightarrow {}^7F_2$ transition. The period of pulse reception display was evaluated longitudinal velocity (V_L) and shear velocity (V_S) [13].
This relation was used to obtain the ultrasonic velocity

$$V_L = \frac{2d}{\Delta t} \quad (1)$$

$$V_S = \frac{2d}{\Delta t} \quad (2)$$

Glass width is symbolized with d and Δt is the period gap.

The elastic modulus expressed using Cauchy relation,

$$L = \rho V_L^{\,2} \quad (3)$$

(L) categorised homogenous isotropic material.

$$G = \rho V_S^{\,2} \quad (4)$$

G represent shear resistance.
Bulk modulus (K) represents hydrostatic pressure incompressibility.

$$K = \frac{3L-4G}{3} \quad (5)$$

Young modulus describes stress and strain uniaxial proportionality.

$$E = 2(1+\delta)G \quad (6)$$

Poisson ratio identifies the ratio of axial strain to radial strain (13).

$$\delta = \frac{L-2G}{2(L-G)} \quad (7)$$

Poisson's ratio (δ) were analysed via equation (7).

Table 2 depicts ultrasonic values increasing with a proportionate increase in AgNPs contents ascribed to the reduction in a non-bridging oxygen and glass connectivity network rise [14]. The rise in elastic moduli through increase AgNPs contents reveals a shift in network bonds per unit volume presence. GC_{12} the ratio describes the dimensionality of the glass system and field force character [15] [16]. If GC_{12}= is said to be central when the value is 1 and non-central when its $GC_{12}\neq 1$. The observed range of values is from 0.8350 to 0.8916 (Table 2), implying central forces as a result of diminishing bond fraction [11] [17].

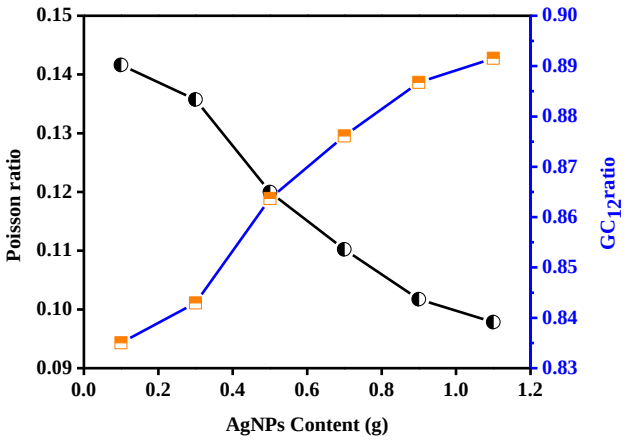

Figure. 2 $\mathbf{GC_{12}}$ratio versus Poisson ratio against AgNPs Contents

The Poisson ratio from (0.1 to 0.2) indicate higher cross-link density but (0.3 to 0.5) reveal lower cross-link density [11]. Poisson ratio is calculated from ultrasonic velocity in which they diminution trend as AgNPs contents increases from (0.0978 to 0.1416) as displayed in (Figure 2) [18]. Poisson ratio depicts an obvious connection with cross-link density as portrayed by the amount of bridging bonds per cation [19].

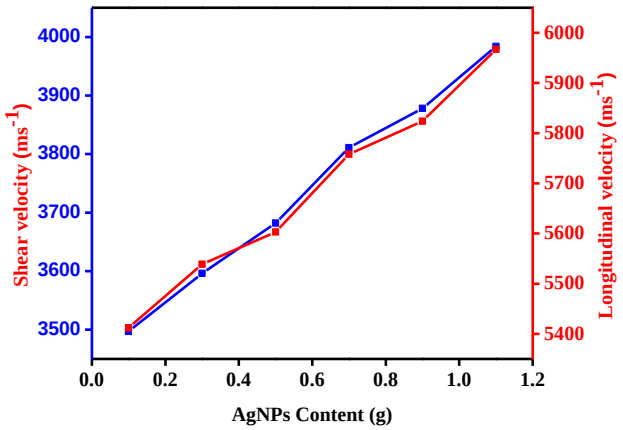

Figure. 3 Shear and longitudinal velocities against AgNPs contents

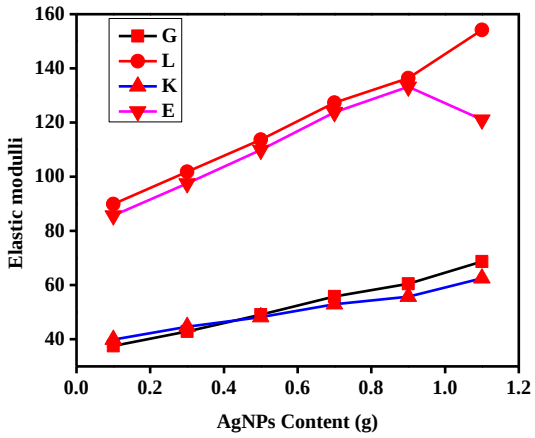

Figure 4. Elastic moduli variation with AgNPs contents

Hardness is expressed as the mean pressure material support under load [20]. This is determined by the relation.

$$HV = \alpha \frac{F}{d_2} \quad (8)$$

Therefore, α is the indenters geometrical constant (0.1891) F is the applied load (N) and d_2 is indenters diagonals. Fig. 5 shows a linear increase of hardness with increase AgNPs contents.

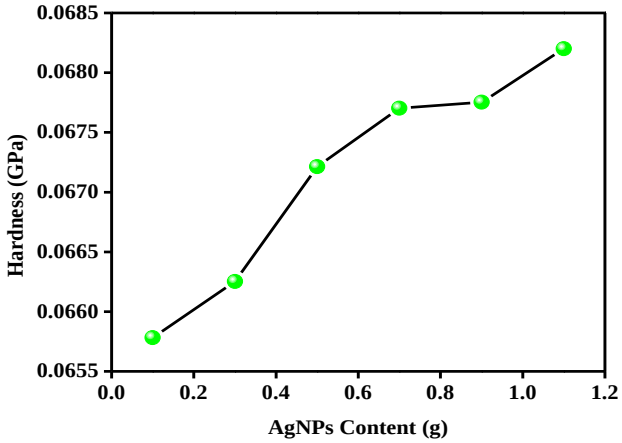

Figure 5 Hardness against AgNPs content

Table 1 Vickers hardness of the synthesized glasses against AgNPs contents

Glass system	Hardness ±0.0020	D1 ±0.0016	D2 ±0.018	HV(GPa) ±0.004
EPMZAg0.1	360	140	141	0.0658
EPMZAg0.3	361	139	140	0.0663
EPMZAg0.5	363	139	138	0.0672
EPMZAg0.7	370	137	137	0.0677
EPMZAg0.9	373	137	137	0.0678
EPMZAg1.1	386	136	136	0.0682

Table 2. Experimental values of Elastic moduli in comparison with existing literature

Glass code	V_L (ms^{-1})	V_S (ms^{-1})	Elastic moduli L GPa	G GPa	K GPa	E GPa	σ	GC_{12}	Ref.
EPMZAg0.1	5412	3497	89.91	37.54	39.86	85.72	0.1416	0.8350	Present work
EPMZAg0.3	5539	3596	101.85	42.93	44.61	97.52	0.1357	0.8430	Present work
EPMZAg0.5	5603	3682	113.64	49.07	48.21	109.92	0.1200	0.8637	Present work
EPMZAg0.7	5758	3811	127.31	55.77	52.95	123.83	0.1102	0.8761	Present work
EPMZAg0.9	5824	3878	136.35	60.45	55.74	133.21	0.1017	0.8868	Present work
EPMZAg1.1	5967	3984	154.17	68.72	62.53	150.89	0.0978	0.8916	Present work
TiB_2	-	-	-	-	-	55	0.18	-	[1]
SiO_2	6440	3923	106.30	39.44	53.70	95.06	-	-	[5]
NPC	4101	2500	48.45	15.69	27.53	39.6	0.261	0.92	[11]
BTDCe4	4476	2230	64.251	15.948	43.040	42.581	0.335	-	[13]
NDF3	-	-	104	-	61	82			[19]
SHA	-	-	-	-	-	27.3	-	-	[20]

Figure 6 illustrates the evaluated CIE chromaticity coordinates of the synthesized glasses with values obtained within the NTSC accepted range for red Phosphor ($x = 0.67, y = 0.33$) [21][22]. This assertion confirms the suitability of the glasses in red laser application [23].

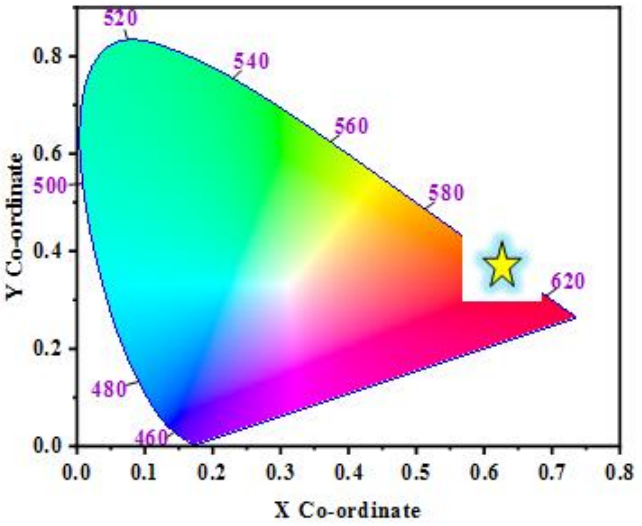

Figure 6. The CIE chromaticity diagram of the synthesized glasses

4. Conclusion

The first-time mechanical properties of silver nanoparticle sensitized phosphate glasses were evaluated. The monitored rising trend of longitudinal velocities and shear velocities were ascribed to glass compactness and network structure. The increase in nanoparticles contents attributes to the rise in Poisson's ratio, elastic moduli, and density cross-link. This evidence signifies the rise of the rigidity of the glass network matrix. It further reveals the high stability and appreciable mechanical trait in the glass matrix. The achieved high quantum efficiency ($\eta = 97.9\%$) of the synthesized Au0.30 sample glass significantly enhanced photoluminescence intensity for the red peak. This enhancement can be an excellent composition for red lasing.

Acknowledgments
The authors are grateful to Sokoto Energy Research Center, Usmanu Danfodiyo University Sokoto and Tertiary Education Trust Fund (TETFUND) Nigeria

References

1. Yonezu A, Xu B, Chen X. Indentation induced lateral crack in ceramics with surface hardening. Mater Sci Eng A. 2009;507(1–2):226–35.
2. Yang YJ, Cheng BY, Lv JW, Li B, Ma MZ, Zhang XY. Effect of Ag substitution for Ti on glass-forming ability, thermal stability and mechanical properties of Zr-based bulk metallic glasses. Mater Sci Eng A. 2019;746(October 2018):229–38.
3. Al-Amri A, Evans JT. Degradation of the strength of glass after light contact with other materials. Mater Sci Eng A. 1994;177(1–2):11–8.
4. Jupri SA, Ghoshal SK, Omar MF, Yusof NN. Spectroscopic traits of holmium in magnesium zinc sulfophosphate glass host: Judd – Ofelt evaluation. J Alloys Compd. 2018;753:446–56.
5. Laopaiboon R, Bootjomchai C. Characterization of elastic and structural properties of alkali-borosilicate glasses doped with vanadium oxide using ultrasonic technique. Glas Phys Chem. 2015;41(4):352–8.
6. Sawamura S, Wondraczek L. Scratch hardness of glass. Phys Rev Mater. 2018;2(9).
7. A.A. Salim, S.K. Ghoshal, G. Krishnan, H. Bakhtiar, Tailored fluorescence traits of pulse laser

ablated Gold-Cinnamon nanocomposites, Mater. Lett. 264 (2020) 127335..
8. Gopi S, Jose SK, George A, Unnikrishnan N. V, Joseph C, P.R.Biju. Luminescence and phonon sideband analysis of - Eu^{3+} doped alkali fluoroborate glasses for red emission applications. J Mater Sci Mater Electron. 2018;29(1):674–82.
9. Danmallam IM, Ghoshal SK, Ariffin R, Jupri SA, Sharma S, Bulus I. Judd-Ofelt evaluation of europium ion transition enhancement in phosphate glass. Optik (Stuttg). 2019;196(July):163197.
10. Danmallam IM, Ghoshal SK, Ariffin R, Jupri SA, Sharma S. Europium ions and silver nanoparticles co-doped magnesium-zinc-sulfophosphate glasses: Evaluation of ligand field and Judd-Ofelt parameters. J Lumin. 2019;116713.
11. Marzouk SY. Ultrasonic and infrared measurements of copper-doped sodium phosphate glasses. Mater Chem Phys. 2009;114(1):188–93.
12. Mohammed I, Krishna S, Ariffin R. Controlled physical and optical traits of magnesium-zinc sulphophosphate glass : role of europium ions. Malaysian J Fundam Appl Sci. 2018;463–7.
13. Bulus I, Hussin R, Ghoshal SK, Tamuri AR, Jupri SA. Enhanced elastic and optical attributes of boro-telluro-dolomite glasses: Role of CeO_2 doping. Ceram Int. 2019;(June):0–9.
14. Gong J, Wu J, Guan Z. Examination of the indentation size effect in low-load vickers hardness testing of ceramics. J Eur Ceram Soc. 1999;19(15):2625–31.
15. Saddeek YB. Ultrasonic study and physical properties of some borate glasses. Mater Chem Phys. 2004;83(2–3):222–8.
16. Renjo MM, Ćurković L, Štefančić S, Ćorić D. Indentation size effect of Y-TZP dental ceramics. Dent Mater. 2014;30(12):371–376.
17. A.A. Salim, S.K. Ghoshal, H. Bakhtiar, G. Krishnan, M. Safwan Aziz, H.H.J. Sapingi, Pulse laser ablated growth of Au-Ag nanocolloids: Basic insight on physiochemical attributes, J. Phys. Conf. Ser. 1484 (2020).
18. Bridge B, Higazy AA. Acoustic and optical Debye temperatures of the vitreous system CoO-Co_2O_3-P_2O_5. J Mater Sci. 1986;21(7):2385–90.
19. Marzouk SY, Zobaidi S, Okasha A, Gaafar MS. The spectroscopic and elastic properties of borosilicate glasses doped with NdF3. J Non Cryst Solids [Internet]. 2018;490(January):22–30.
20. Roop Kumar R, Wang M. Modulus and hardness evaluations of sintered bioceramic powders and functionally graded bioactive composites by nano-indentation technique. Mater Sci Eng A. 2002;338(1–2):230–6.
21. A.A. Salim, S.K. Ghoshal, N. Bidin, H. Bakhtiar, Akademia Baru Environmental-Amiable Pulsed Laser Ablation in Liquid Mediated Growth of Silver / Cinammon Nanocomposites : Absorption Attributes Akademia Baru, 1 (2018) 28–33.
22. A.A. Salim, N. Bidin, A.S. Lafi, F.Z. Huyop, Antibacterial activity of PLAL synthesized nanocinnamon, Mater. Des. 132 (2017) 486–495.
23. A.A. Salim, N. Bidin, S.K. Ghoshal, Growth and characterization of spherical cinnamon nanoparticles: Evaluation of antibacterial efficacy, LWT - Food Sci. Technol. 90 (2018) 346–353.